11TH SYMPOSIUM ON COMPOSITE MATERIALS: TESTING AND DESIGN

Authors: Henjen Ho[1], Haryanto T. Budiman[1], Ming-Yi Tsai[1], John Morton[1], and Gary L. Farley[2]

Title: Composite Material Shear Property Measurement Using The Iosipescu Specimen

Authors' Affiliations: [1]Visiting Assistant Professor, Graduate Research Assistant, Research Associate, Professor, respectively, Department of Engineering Science and Mechanics, Virginia Polytechnic Institute and State University, Blacksburg, VA 24061-0219. (H.T. Budiman is currently a Ph.D. student at Department of Aeronautics and Astronautics, MIT, Cambridge, MA 02139). [2]Research Scientist, US Army Aerostructures Directorate, NASA Langley Research Center, Hampton, VA 23665-5225.

ABSTRACT: A detailed evaluation of the suitability of the Iosipescu specimen tested in the modified Wyoming fixture is presented. Finite element analysis and moire interferometry are used to assess the uniformity of the shear stress field in the test section of unidirectional and cross-ply graphite-epoxy composites. The nonuniformity of the strain field and the sensitivity of some fiber orientations to the specimen/fixture contact mechanics are discussed. The shear responses obtained for unidirectional and cross-ply graphite-epoxy composites are discussed and problems associated with anomalous behavior are addressed. An experimental determination of the shear response of a range of material systems using strain gage instrumentation and moire interferometry is performed.

KEY WORDS: Iosipescu specimen, shear modulus, graphite-epoxy, woven fabric, particulate composite, sheet molding compound.

Introduction

The Iosipescu specimen was originally proposed for the shear strength measurement of metals by Nicolae Iosipescu [1] in the 1960's. In the late 1970's, Walrath and Adams [2] developed the Wyoming fixture (W1) and specimen based upon Iosipescu's original concept. Further research by Adams and Walrath [3,4] on the test geometry and test fixture resulted in the production of a modified Wyoming fixture (W2) and specimen which had a larger test section and larger specimen-fixture load introduction regions, as shown in Fig.1.

The advantages of the Iosipescu shear test method as compared with other shear test methods are (1) its small specimen size, (2) the ability to evaluate different specimen thicknesses, (3) the ability to test a wide range of material forms (such as isotropic and orthotropic materials, composite materials with continuous and discontinuous fibers, and composite materials with different fiber orientations), (4) the capability for measuring shear properties in the 1-2, 1-3 and 2-3 material planes and (5) the potential for measuring shear modulus and shear strength. These attractive features of the Iosipescu shear test method have resulted in its wide use by the composite materials industry. Unfortunately, some problems associated with the experimental results have been identified [5-7]. These problems are (1) an impure shear state in the test section for 0° specimens, and (2) the large differences in the shear stress-strain responses obtained from 0°, 90° and 0°/90° specimens, as shown in Fig.2. Note that the 0° and 90° fiber directions are defined in Fig.1b.

The objective of this paper is to describe the response mechanisms associated with the impure stress state and the anomalous shear stress-strain response, and to illustrate their relative importance in a wide variety of composite material systems. The experimental results are presented to assist in describing the fundamental response mechanisms and to identify any special precautions which are to be recommended for reliable shear property measurement.

Shear Stress State in the Test Section

Numerical [3, 9] and experimental [6,10,11] stress analyses have been used to evaluate the purity and uniformity of the shear stress field in the test section of composite Iosipescu specimens. It has been shown that the shear stress state developed in the specimen test section depends upon the material orthotropic ratio (E_x/E_y). This effect is illustrated through a numerical analysis following an iterative scheme developed by Ho *et al.* [8] and using material property data [12] shown in Table 1. Since the stress state in the test section is not uniform and strains are measured using a small strain gage rosette located at the center of the specimen, it is convenient to present the shear field in the specimen test section as distributions of shear strain across the notches of the specimen, and to normalize the strains with respect to the average shear strain γ_{avg} between the notches. Where

$$\gamma_{avg} = \frac{1}{h}\int_{-\frac{h}{2}}^{\frac{h}{2}} \gamma_{xy} \, dy \qquad (1)$$

and h is the distance between the notch roots. In Fig. 3 the shear strains distributions obtained for unidirection (0° and 90°) and cross-ply (0°/90°) graphite-epoxy composites are presented. The shear strain distributions across the notches are not uniform and the distributions are of different shapes for 0°, 90° and 0°/90° specimens. Moire interferometry has also been used to determine the shear strain distributions between the notches [6,10,11] from the test section surface displacement components (u,v). Typical moire fringe patterns from 0° and 90° graphite-epoxy specimens are shown in Fig.4. The fringes are adjusted such that the u-field contains minimum fringes and most deformation information is contained in the v-field. The zig-zag pattern in the u-field of the 0° specimen and the fringe bands in the v-field of the 90° specimen suggest that the material cannot be regarded as homogeneous [10] as assumed in the numerical analysis. The normal strains are readily interpreted in terms of the gradients of the fringe contours, in the u field patterns in the x-direction (horizontal), $\partial u/\partial x$, and, in the v field patterns in the y-direction (vertical), $\partial v/\partial y$.

Calculation of the shear strains requires the cross derivatives in both fringe patterns. The v-displacement field for the 0° specimen reveals that they are S-shaped such that there is a vertical gradient corresponding to a normal strain ε_y. The v-displacement field for the 90° specimen, shown in Fig.4b, consists of almost straight vertical fringes. Along the line between the notches and in the center of the test section where strain gages are normally applied, the normal strain ε_y is zero. Shear strain distributions obtained from the moire displacement data are shown in Fig.5. The experimentally determined shear strain distributions are similar in form to the distributions obtained from the numerical analysis as presented in Fig.3. The data in Fig. 5 correspond to several load levels. In the case of the 0° graphite-epoxy specimen the shear strain distribution is sensitive to the load level, particularly near the notch root, and the distribution at the lower load level is not symmetric. The lack of smoothness in the experimentally determined shear strain distributions is due to a degree of nonuniformity of the material and numerical errors in determining the shear strains which are obtained by differentiating the displacement data from the moire experiment [10].

The normal strain distributions obtained from the numerical analyses are also shown in Fig. 3. In the ideal case of pure shear the longitudinal (ε_x) and transverse (ε_y) strains should be zero in the specimen test section. In the cases of the 90° and 0°/90° graphite-epoxy pure shear is very nearly attained in the numerical model. However, the 0° specimen suffers from significant (compressive) normal strains (ε_y), Fig.3a. This effect is due to the diffusion of the load introduced by the fixture into the specimen test section. This load proximity effect is greatest in highly orthotropic materials when the extensional stiffness in the direction of the specimen x-axis is greater than that in the transverse y-direction [10]. The presence of the normal strain in the test section causes the strain gages at ±45° to record unequal values. Sullivan [13] stated that "In a properly loaded Iosipescu specimen, the two strains at ±45 deg should be equal in magnitude and opposite in sign to a reasonable approximation." Lee and Munro [14] showed recently that this condition cannot be achieved experimentally for 0° specimens. The numerical model [8] can be used to determine the strains that would be recorded by individual gages at ±45° to show that the phenomenon can be

attributed to the presence of transverse normal strains in the specimen gage section and is an inherent property of the 0° specimen. Simulated individual gage readings for 0°, 90° and 0°/90° specimens are shown in Fig.6 for graphite-epoxy composite. It is shown that for 90° and 0°/90° specimens, the magnitude of the compressive strain in the +45°gage is approximately equal to the magnitude of the tensile strain in the -45° gage. But for the 0° specimens, the compressive strain in the +45° gage is larger in magnitude than the tensile strain in the -45° gage. The ratio of the tensile strain to compressive strain, as recorded by the ±45° gages, is found to be 0.6 for graphite-epoxy composite. Though the two gages in the 0° specimen do not record equal and opposite strains, the shear strain still can be calculated by

$$\gamma_{12} = SG1 - SG2 \tag{2}$$

(where SG1 and SG2 are the strains in the ±45° gages) as long as the normal strains are uniformly distributed in the gage section [8]. Experimental confirmation of the individual strain gage behavior is shown in Fig. 7 in which the ±45° gage reading are very nearly equal and opposite for the 90° and 0°/90° graphite-epoxy specimens but not for the 0° specimen.

The numerical analyses can be used to demonstrate the sensitivity of the shear strain distributions in the test section to material orthotropy ratios. It is shown in Fig.8 that for material with higher orthotropic ratio, such as graphite-epoxy, the shear strain distribution is more nonuniform than material with lower orthotropic ratio, such as glass-epoxy. The shear strain at the specimen center does not equal the average shear strain across the notches. Therefore, when strain gages are located at the center of the specimen, correction factors must be applied to the shear strain, γ_{gage}, measured by the strain gages to determine the average shear strain, γ_{avg}, across the notches in the calculation of shear modulus [8-10,15]. The shear modulus G_{12} is determined by

$$G_{12} = \tau_{avg} / \gamma_{avg} = (P/A) / (\gamma_{gage} / CF) = CF \times G^* \tag{3}$$

where τ_{avg} is the averaged shear stress across the notches, CF is the correction factor, G* is the apparent shear modulus, P is the applied load and A is the cross-sectional area between the notches. Approximately, the correction factors can be expressed as [8]

$$CF = 1.036 - 0.125 \times \log(E_x/E_y) \tag{4}$$

where E_x and E_y are extensional stiffnesses in the longitudinal and transverse directions, respectively.

Due to the fixture design and possible material nonhomogeneity, the load transfer mechanism between fixture and specimen may not be unique between specimens. The effect of load points on the shear strain disbribution along the notch axis has been evaluated [8,15]. It was found that the shear stress distribution across the notches for the 90° specimen is not sensitive to the load transfer mechanism. But the shear field for the 0° specimen is sensitive to how the load is transferred to the specimen from the fixture. In practice the specimen-fixture contact mechanism may differ based on specimen-to-specimen variation. The consequence of the sensitivity of the 0° specimen to load application points is that the shear moduli of the 0° specimens may vary from specimen to specimen.

In summary, the shear stress state produced in the specimen test section is material dependent, and for a given orthotropic material, the distribution depends upon the orientation of the the stiffer material axis relative to the specimen axis. When the orthotropic ratio is high and the extensional stiffness is larger in the direction of the specimen axis, the ±45° elements of a strain gage rosette will not be equal and opposite, and the shear strain field between the notch roots will not be pure. The lack of a pure shear field in the test section does not affect the shear modulus determination and the shear strain can be determined from the ±45° gage readings in the same way as for the pure shear field. In order to obtain consistent shear modulus values correction factors must be applied to the apparent shear modulus to account for the nonuniform shear fields. The

case of 0°/90° laminates is approximately midway between that of the 0° and 90° cases. For cross-ply specimens the corrected shear modulus will be about 4% higher than the apparent value.

Anomalous Shear Stress-Strain Responses

The shear stress-strain responses for 0°, 90° and 0°/90° specimens should be the same. The data presented in Fig. 2 do not correspond to apparently identical shear stress-strain responses since the shear strain distributions in the test section are different for the three cases and the average shear stress is plotted against the local shear strain obtained from the strain gages. If the average shear strain is determined (experimentally or numerically) almost coincident responses can be obtained [16].

The response for the 90° specimen could be different to that shown in Fig.2 if a strain gage rosette were used on one face of the specimen, as is commonly used. If two strain gages rosettes were used back-to-back the shear strains recorded from each rosette could be quite different and anomalous shear stress-strain reponses would be obtained if the data from one of the rosettes were used. Morton *et al.* [15] have shown that the differences in the strain gage rosette data is caused by twisting of the 90° specimen. Twisting was also detected in the cross-ply graphite-epoxy specimen but not in the 0° specimen. For back-to-back strain gage rosettes it was found that the effect of twisting upon the shear stress-strain response could be eliminating by taking the average of the shears strains form each rosette. An illustration of the way in which specimen twisting can lead to anomalous shear stress-strain responses is presented in Fig.9a which contains data from a 90° graphite-epoxy specimen which has been loaded, unloaded and loaded in various positions in the fixture. The effect of plotting the average shear stress against the average of front and back surface shear strain data in Figs.9a is shown in Figs.9b in which a unique response is indicated.

It should be noted that the 90° specimen in Fig. 3 fails at a much lower shear stress than the 0° and 0°/90° specimens. Thus an anomaly in the shear stress-strain response of the 90° specimen will appear even after correcting for the nonuniform strain distributions in the specimen test section in the form of apparently premature failure compared to the 0° and 0°/90° specimens. Twisting is

partly responsible for this effect since the shear strains on one surface of the specimen will be higher than on the other, and of course higher than the average of the front and back surface shear strains used for the responses. Failure would then occur under combined mode II and mode III. The effect of twisting can be significantly reduced by applying a soft layer being the specimen and the fixture, and the shear stress at failure is increased correspondingly. It is noted, however, that failure does not initiate at the minimum specimen cross-section [8] but at the junction between the notch root and flank where significant stresses (σ_x) transverse to the fiber direction occur [8]. Failures in the 90° specimens will then occur under a complex combination of modes I, II and III. In the case of the 0° specimen failure may also be initiated at the junction between the notch root and flank. However, specimen failure may not occur and the shear stress-strain response may continue to rise with the applied shear stress in a smooth manner, as a network of cracks parallel to the fibers develop in the test section. In the 0° specimen failure initiates under combined mode I and II. Since the 0°/90° specimen also twists and develops a network of cracks in the late stages of loading, failure will also occur in a complex mode. In none of these specimens does failure occur in a pure shear mode so the maximum shear stress cannot be taken to represent the shear strength of the material. Furthermore, the correction factors developed to account for the nonuniform shear strain state were derived for linear elastic conditions. Material and geometric nonlinearities will lead to stress redistribution and futher corrections would have to be made if the true material response is to be obtained.

The stress state in the 0° graphite-epoxy specimen is sensitive to the exact interaction between the specimen and fixture. In practice, this sensitivity will lead to variations in the shear stress-strain response of apparently identical specimens. It is not clear that this sensitivity can be reduced other than by seeking unrealistic levels of material uniformity.

Shear Response Data of Some Material Systems

An important feature of the Iosipescu specimen is the potential to measure the shear properties of a wide range of material systems. The performance of unidirectional graphite-epoxy Iosipescu specimens tested in the modified Wyoming fixture has been used to illustrate some problems and possible remedies. The nature of the problems is such that they are of greater or lesser importance for different material systems. Key features of the shear response of a range of material systems will be outlined. The material systems are:

(i) Graphite-epoxy woven fabric composites

(ii) Epoxy based aluminum particulate composite

(iii) Sheet molding compound

(iv) Aluminum alloy.

The performance is assessed in terms of conventional strain gage instrumentation and comparison with moire interferometry. Generally, six strain gaged and two moire specimens were prepared and tested according to the procedure suggested by Ho *et al.* [17]. For the strain gaged specimens, strain gage rosettes were attached to the specimen on the front and back faces.

Graphite-epoxy woven fabric composites

Five graphite/3501-6 epoxy woven fabric panels were tested . The weave architectures investigated were a 3k AS4 $[0/90]_{7s}$ uniweave [panel 1], a 3k Celion $[0/90]_{6s}$ plain weave [panel 2], a 12k AS4 $[0/90]_{2s}$ plain weave [panel 3], a 3k Celion $[0/90]_{4s}$ 5-harness satin weave [panel 4] and a 3k Celion $[0/90]_{3s}$ 8-harness satin weave [panel 5]. The number of plies in each laminate differed so that the laminate thicknesses (3.8mm) were nominally the same. A summary of these five panels is presented in Table 2.

Shear stress-strain response--The shear stress-strain data obtained from the strain gaged specimens for the five panels are shown in Figs.10a-e. To eliminate the effect of specimen twisting [15] on shear modulus, the average of the front and back shear strains was determined.

The shear stress-strain response for these 5 materials are highly nonlinear with linear response typically below 0.5 percent shear strain. A 0.2% secant shear modulus was used to determine the shear modulus. All fabrics exhibited some twisting because of the 90° fibers [18]. The shear stress-strain response for all specimens of the same material was consistent except for one specimen from panel 2 and all of panel 3. The deviation in response of the panel 2 specimen was due to nonuniform specimen thickness. In panel 3 (plain weave $[0/90]_{2S}$) the shear stress-strain data for the six strain-gaged specimens were inconsistent. The shear moduli and strengths together with the corresponding standard deviations for the five material systems are shown in Table 3. Since fiber volume fractions of the five material systems are different, a direct comparison of the shear moduli and strengths of the five material systems cannot be made and is not attempted here. The standard deviation of the large filament count yarn (12k) AS4 plain weave fabric composite (panel 3) is higher than the other smaller filament count yarn fabric composites. This is attributed to the larger resin rich regions between the large filament count yarns. The mechanisms responsible for this large variation will be discussed in a subsequent section.

Displacement and strain field in test section--Nonuniform u- and v-displacement fields in the test section were observed for specimens from all panels [18]. Typical u- and v-fields of specimens from panel 3 and panel 4 are shown in Fig.11. The shear strain distribution between the notches obtained from moire data reduction was nonuniform for all specimens, as seen in Fig.12. From Fig.12, the shear modulus correction factors determined experimentally are 1.01, 1.02, 1.12, 0.99 and 0.98 for specimens from panels 1 to 5, respectively. The shear modulus correction factors are close to unity except for the large tow sized specimen in which the shear strain distribution in the test section is highly nonuniform and specimen dependent.

High-density fringe bands were observed in the u- and v-displacement fields, Fig.11. This phenomenon is attributed to the nonuniformity of fiber volume fraction which is an artifact of the textile architecture. Resin rich regions between the yarns create variations in local shear stiffness resulting in these bands. Furthermore, the observed number of fringe bands across the test section

is in agreement with the number of yarns in the test section [18]. A consequence of the nonuniform shear strain field is the potential inaccuracy in measuring the strain using strain gages. The strain measured by a strain gage covering a region composed of primarily a single yarn would be different if the same gage was positioned primarily over a resin rich region.

An artifact of textile architecture of woven materials is the size of the repeating cell and yarn diameter relative to the size of the specimens test section and the low probability of obtaining the same portion or number of unit cells in the test section of specimens from the same panel, see Figs.11a & c. All of these factors can cause considerable variability in the measured response. Therefore, it may be necessary to develop a larger specimen and fixture, and use large sized strain gages for the mechanical testing of textile composite materials.

Epoxy based aluminum particulate composite

The epoxy based aluminum particulate composite was used as potted end support for graphite-epoxy Z-section stiffeners loaded in compression [19]. The extensional modulus and Poisson ratio were measured as E=7.75 GPa and ν=0.43 [19].

Typical u- and v-field moire fringe patterns are shown in Figs.13a&b. In the u-field, shear strain component $\partial u/\partial y$ in the gage section is essentially negligible but are of significant magnitude at the notches. At the right flank of the bottom notch, tensile ε_x is observed. In the v-field, the fringes are not straight in the test section and a small amount of ε_y exists. The existence of ε_y is due to the low extensional modulus of this particulate composite. The shear strain distribution across the notches obtained from the moire data reduction is shown in Fig.13b. It is found that the shear strain distribution is approximately uniform except at the notch regions. The shear strain at the center of the test section is about 0.94 to 1.02 γ_{avg} for all shear strain levels. Under low loading, the shear strain distribution shows more fluctuations. The behavior of this particulate composite specimen is similar to that of the 0° graphite-epoxy specimen due to the common characteristic of low transverse stiffness. From this experiment, the secant shear modulus at γ_{xy} =0.15% was 2.4 GPa. If E and ν values are substituted into G=E/2(1+ν), a shear modulus G=2.7

GPa is obtained. Thus this epoxy based aluminum particulate composite can be regarded as an isotropic material.

Sheet molding compound (SMC)

The uniformity of the shear field of the SMC composite was evaluated based on the full field moire fringe patterns. Also, the directionality in the mechanical properties of the SMC materials as a result of the single-direction movement of the pressing rollers in the manufacturing process was investigated. Specimens were cut from a panel at different relative orientations (0°, 30°, 45°, 60° and 90°) with respect to a reference axis [20].

The shear responses for specimens cut from different orientations in the same panel are shown in Fig.14a. The shear behavior of the SMC composite is highly nonlinear with regions of linearity up to 0.3% shear strain. The corresponding shear moduli are shown in Fig.14b. The shear modulus varies with specimen orientation. There also exists some scatter, ranging from 3% to 13%, in the experimental data for specimens from different orientations. Moire experiments performed on the SMC specimens also detect the effect of different relative specimen orientations on the mechanical properties [20]. As the relative orientation angle increases from 0° to 90°, the v-field of the corresponding specimens becomes less S-shaped [20]. The moire fringe patterns for a specimen of 0° relative orientation are shown in Fig.15a. The normalized shear strain distribution across the notches obtained from the moire data reduction for 0° relative orientation is shown in Fig.17b. Depending on the relative orientation, the shear strain distributions are of different shape [20], which further provide evidence of the direction dependence of the SMC composite materials.

Aluminum alloy

For isotropic materials it is not necessary to use the Iosipescu specimen for shear modulus measurement since tensile test data can be used to determine the shear modulus. It should be recalled that the original Iosipescu specimen was developed for shear strength measurement of metals. Data for the shear stress-strain response of an aluminum alloy Iosipescu specimen are

presented in Fig.16a in which the shear strains were taken from a single specimen and a single strain gage rosette. Significant twisting is apparent from the responses shown in Fig.16. Averaging sets of shear strain data corresponding to pairs of front and back surface shear strains eliminates the effect of twisting upon the shear stress-strain response as shown in Fig.16b. The behavior of the aluminum alloy specimen should be contrasted with the nearly-isotropic SMC and aluminum filled epoxy specimens which showed little or no evidence of twisting.

Conclusions

The problems associated with the Iosipescu shear test have been identified and demonstrated numerically and experimentally. The presence of transverse normal strains in the test section of the specimen is due to the low transverse stiffness of the specimen, such as 0° graphite-epoxy, SMC and epoxy based aluminum particulate composites. The lack of pure shear results in unsymmetric strain gage readings in the ±45° gages but does not affect accurate shear strain measurement as long as the normal and shear strain fields are uniform. However, sensitivity of the specimens of low transverse stiffness to the load transfer mechanics is an inherent property, which will cause variations in the measured shear modulus. Specimen twisting is a result of the fixture design and high transverse stiffness of the specimens. The effect of specimen twisting on shear modulus measurement is eliminated if average of front and back shear strains is taken. Shear modulus measurement using strain gages is not accurate for the woven fabric composites when the fiber tow size is large. The shear properties of the SMC material is direction dependent. In general, the application of Iosipescu shear test to composite shear modulus measurement is very accurate if the appropriate instrumentation and data reduction methods are used.

Acknowledgement

The financial support from the US Aerostructures Directorate (under NASA Research Grant NAG-1-1053) and the Virginia Tech NSF Center for High Performance Polymeric Adhesive and Composites (under NSF Grant Number DMR 8809714) is gratefully acknowledged. The authors

would also like to express their gratitude to Drs. Robert Czarnek and Joosik Lee, Mr. Shih-Yung Lin of the Engineering Science and Mechanics Department at VPI&SU for their assistance with the moire experiments.

References

[1] Iosipescu, N., "New Accurate Procedure for Single Shear Testing of Metals," *Journal of Materials*, 2 (3) : 537-566 (1967).

[2] Walrath, D.E. and Adams, D. F., "The Iosipescu Shear Test As Applied to Composite Materials," *Experimental Mechanics*, 23 (1) : 105-110 (1983).

[3] Walrath, D.E. and Adams, D. F., "Analysis of the Stress State in an Iosipescu Shear Test Specimen," Report UWME-DR-301-101-1, Department of Mechanical Engineering, University of Wyoming, (June 1983).

[4] Adams, D. F. and Walrath, D. E.,"Further Development of the Iosipescu Shear Test Method,"*Experimental Mechanics* , 27 (2) : 113-119 (1987).

[5] Adams, D. F. and Walrath, D. E.,"Current Status of the Iosipescu Shear Test Method," *Journal of Composite Materials*, 21 (6) : 494-507 (1987).

[6] Abdallah, M. G. and Gascoigne, H. E., "The Influence of Test Fixture Design of Iosipescu Shear Test for Fiber Composite Material," *Test Methods for Design Allowables for Fibrous Composites: 2nd Vol., ASTM STP 1003*, C. C. Chamis, Ed., pp. 231-260 (1989).

[7] Wilson, D.W.,"Evaluation of the V-notched Beam Shear Test Through an Interlaboratory Study", *Journal of Composites Technology and Research*, 12 (3) : 131-138 (1990).

[8] Ho, H., Tsai, M.Y., Morton, J. and Farley, G.L., "Numerical Analysis of The Iosipescu Specimen for Composite Materials," Composite Science and Technology, in press.

[9] Pindera, M. J., Choksi, G., Hidde, J.S. and Herakovich, C.T., "A Methodology for Accurate Shear Characterization of Unidirectional Composites," Journal of Composite Materials, 21 (12) : 1164-1184 (1987)

[10] Ho, H., Morton, J., Tsai, M.Y. and Farley, G.L.,"An Experimental Investigation of Iosipescu Specimen for Composite Materials," Experimental Mechanics, 31 (4) : 328-337 (Dec. 1991).

[11] Pindera, M. J., Ifju. P. and Post, D., "Iosipescu Shear Characterization of Polymeric and Metal Matrix Composites," *Experimental Mechanics*, 30 (1) : 101-108 (1990).

[12] Tsai, S. W. , "Composite Design," 4th edition, Appendix B, p B-2 (1988).

[13] Sullivan, John L., "The Use of Iosipescu Specimens," *Experimental Mechanics*, 28 (3) : 326-328 (1988).

[14] Lee, S. and Munro, M., "Evaluation of Testing Techniques for the Iosipescu Shear Test for Advanced Composite Materials," *Journal of Composite Materials*, 24 : 419-440 (1990).

[15] Morton, J., Ho, H., Tsai, M.Y. and Farley, G.L.,"An Evaluation of The Iosipescu Specimen for Composite Materials Shear Property Measurement," Journal of Composite Materials, 26 (5) : 708-750 (1992).

[16] Ho, H., Tsai, M.Y., Morton, J. and Farley, G.L., " A Comparison of Popular Shear Test Methods for Composite Materials," *Composites Engineering*, in press.

[17] Ho, H., Tsai, M.Y., Morton, J. and Farley, G.L., "An Experimental Procedure for Iosipescu Composite Specimen Tested in Modified Wyoming Fixture," Composites Technology and Research, in review.

[18] Ho, H., Tsai, M.Y., Morton, J. and Farley, G.L., "In-plane Shear Testing of Graphite Woven Fabric Composites," to be submitted to Experimental Mechanics.

[19] Wieland, T., Morton, J. and Starnes, J.H., Jr.,"Scaling Effects in Buckling and Crippling of Graphite-Epoxy Z-Section Stiffners," AIAA/ASME/ASCE/AHS/ASC 32nd Structures, Structure Dynamics and Materials Conference. Baltimore, Maryland, 906-911 (April, 1991).

[20] Budiman, H. T., "An Assessment of Subscale Notched Specimen for Composites Shear Property Measurement," Master Thesis, Department of Engineering Science and Mechanics, Virginia Polytechnic Institute and State University, December, 1991.

Figure Captions

Fig. 1 (a) Modified Wyoming fixture (W2) and (b) modified Iosipescu specimen.

Fig. 2 Typical shear stress-strain data for 0°, 90° and 0°/90° graphite-epoxy specimens.

Fig. 3 Normal and shear strains along the notch axis, normalized with respect to average shear strain, for (a) 0°, (b) 90° and (c) 0°/90° graphite-epoxy specimens.

Fig. 4 U- and v-field moire fringe patterns for (a) 0° and (b) 90° graphite-epoxy specimens.

Fig. 5 Shear strain data across the notches obtained from manual data reduction of moire fringes for (a) 0°, (b) 90° and (c) 0°/90° graphite-epoxy specimens.

Fig. 6 Normalized strains of ±45° gages from finite element analysis for (a) 0°, (b) 90° and (c) 0°/90° graphite-epoxy specimens.

Fig. 7 Strain vs. stress for typical (a) 0°, (b) 90° and (c) 0°/90° graphite-epoxy specimens. Gages are aligned at ±45° and 0° directions.

Fig. 8 Normal and shear strains along the notch axis, normalized with respect to average shear strain, for (a) graphite-epoxy (b) Kevlar-epoxy and (c) glass-epoxy specimens.

Fig. 9 (a) Shear stress-strain data for 90° graphite-epoxy loaded in different orientations which were obtained by rotating the specimen about the x,y and z axis. (b) Average of front and back surface shear strains as a function of shear stress.

Fig. 10 Average of front and back shear stress-strain data of (a) uniweave $[0/90]_{7s}$, (b) plain weave $[0/90]_{6s}$, (c) plain weave $[0/90]_{2s}$, (d) 5HS $[0/90]_{4s}$ and (e) 8HS $[0/90]_{3s}$ specimens.

Fig. 11 Typical moire fringe patterns for (a) plain weave $[0/90]_{2s}$, specimen A, (b) 5HS $[0/90]_{4s}$ and (c) plain weave $[0/90]_{2s}$, specimen B.

Fig. 12 Shear strains across the notches, normalized with respect to the average shear strain, for (a) uniweave $[0/90]_{7s}$, (b) plain weave $[0/90]_{6s}$, (c) plain weave $[0/90]_{2s}$, (d) 5HS $[0/90]_{4s}$ and (e) 8HS $[0/90]_{3s}$ specimens.

Fig. 13 (a) Moire fringe patterns of the epoxy based aluminum particulate composite specimens at an applied load of 476N. (b) Shear strains across the notches, normalized with respect to the average shear strain, for epoxy based aluminum particulate composite specimens.

Fig. 14 (a) Typiccal shear stress-strain response, (b) measured shear modulus for different relative orientations of the SMC-28 specimens.

Fig. 15 (a) Moire fringe patterns, (b) shear strains across the notches, normalized with respect to the average shear strain, of the 0° relative orientation SMC-28 specimen.

Fig. 16 (a) Shear stress-strain data for an aluminum alloy specimen loaded in different orientations which were obtained by rotating the specimen about the x,y and z axis. (b) Average of front and back surface shear strains as a function of shear stress.

Table 1 Mechanical property table for numerical analysis

Material*	E_{11}/E_{22}	G_{12} (GPa)	ν_{12}
epoxy	1.0	1.1**	0.35
steel	1.0	116.3**	0.29
glass-epoxy	4.7	4.1	0.26
Kevlar-epoxy	13.6	2.3	0.34
graphite-epoxy	15.4	7.1	0.30

* Data were obtained from Tsai[12]. ** Calculated using $G = E/2(1 + \nu)$

Table 2 Fabric architechture

Panel Number	Layup	Weave Designation	Weave Architecture (Warp yarns/cm x Fill yarns/cm)	Yarn Description	Fiber Volume Fraction (%)
1	$[0/90]_{7s}$	Uniweave*	7.1	3k AS4	55.4
2	$[0/90]_{6s}$	Plain Weave	4.9 x 4.9	3k Celion	55.5
3	$[0/90]_{2s}$	Plain Weave	3.0x 3.0	12k AS4	52.2
4	$[0/90]_{4s}$	5HS	7.1 x 7.1	3k Celion	59.6
5	$[0/90]_{3s}$	8HS	9.4 x 9.4	3k Celion	51.0

*Uniweave - Approximately 97% of the yarns are orientated in warp direction. A fine denier glass yarn is used in fill direction, 3.1 yarns/cm.

Table 3 Averaged in-plane shear moduli and shear strengths for woven fabric composite materials

Panel Number	Layup	Avg. G_{12} (GPa)	G_{12} Standard Deviation(GPa)	Avg. S_{12} (MPa)	S_{12} Standard Deviation(MPa)
1	$[0/90]_{7s}$	5.33	0.17	136	10.0
2	$[0/90]_{6s}$	4.96	0.25	140	4.1
3	$[0/90]_{2s}$	4.05	0.34	100	2.6
4	$[0/90]_{4s}$	4.69	0.18	142	2.7
5	$[0/90]_{3s}$	4.23	0.06	126	3.7

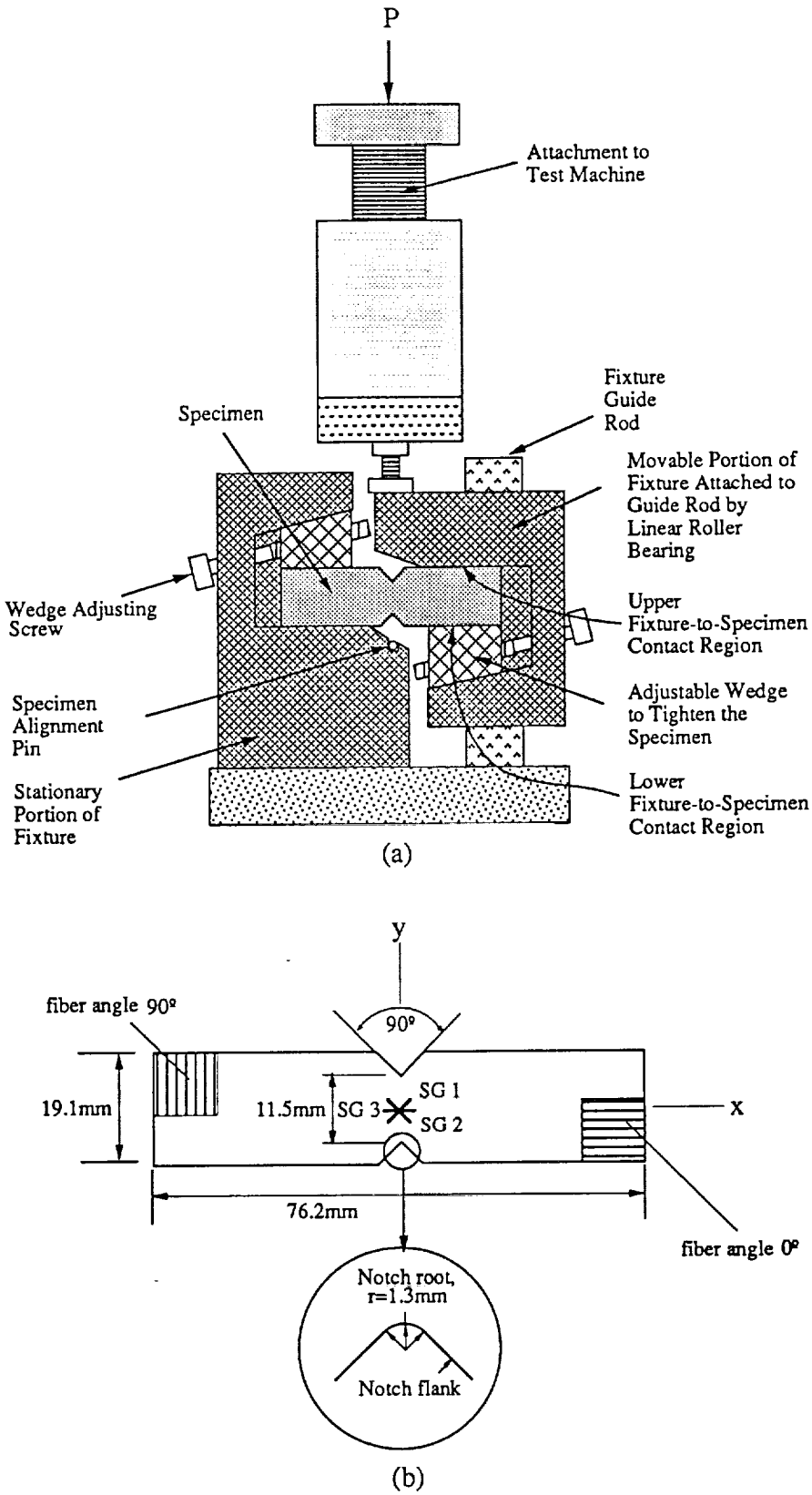

Fig. 1. (a) Modified Wyoming fixture (W2) and (b) modified Iosipescu specimen .

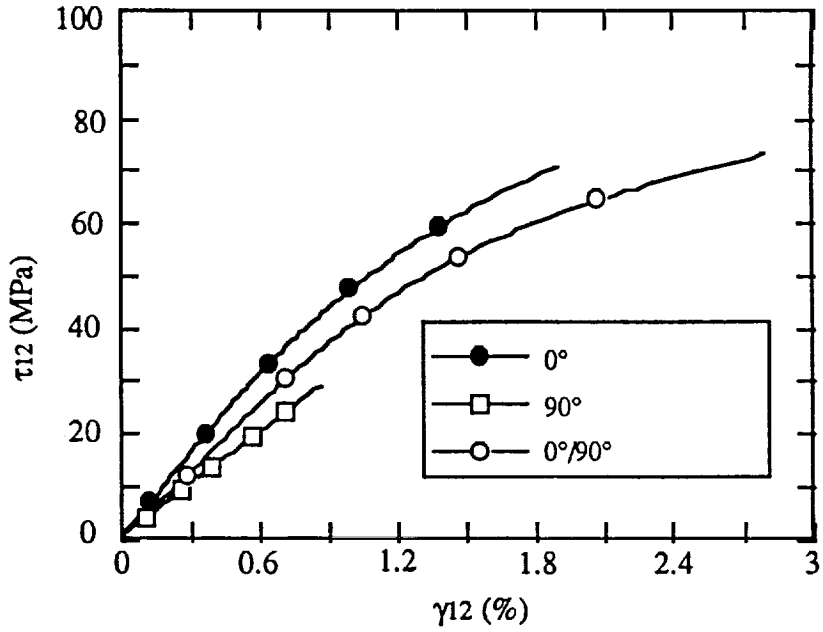

Fig.2. Typical shear stress-strain data for 0°, 90° and 0°/90° graphite-epoxy specimens.

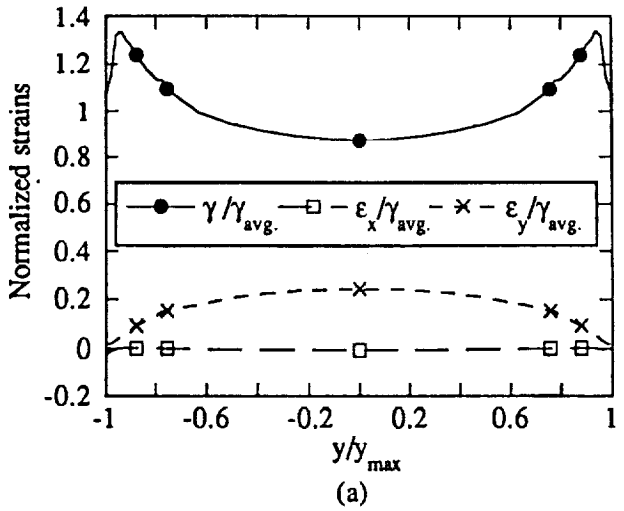

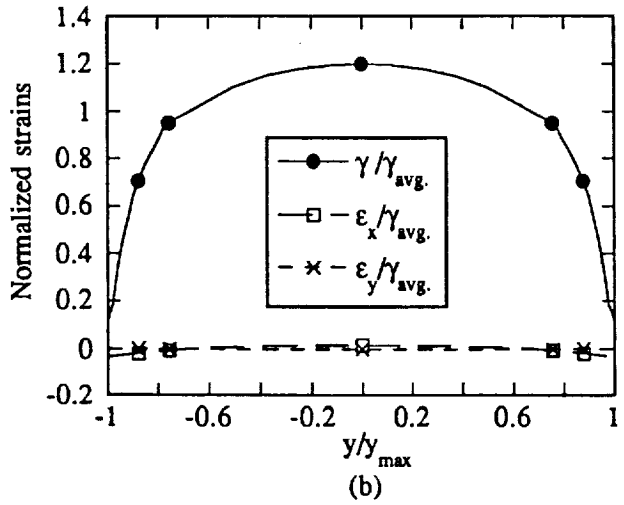

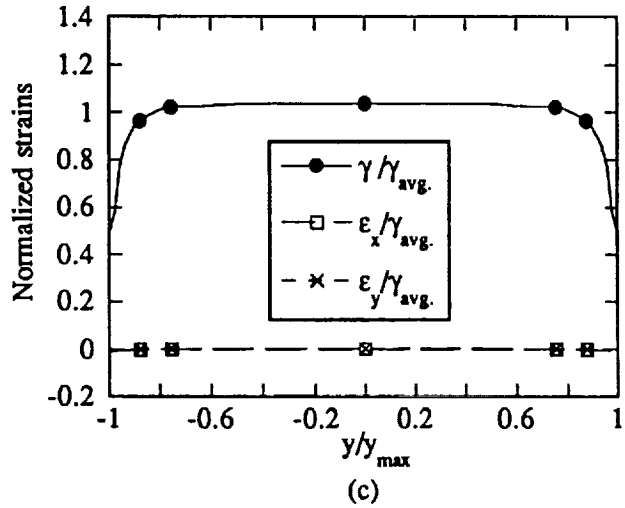

Fig. 3 Normal and shear strains along the notch axis, normalized with respect to average shear strain, for (a) 0°, (b) 90° and (c) 0°/90° graphite-epoxy specimens.

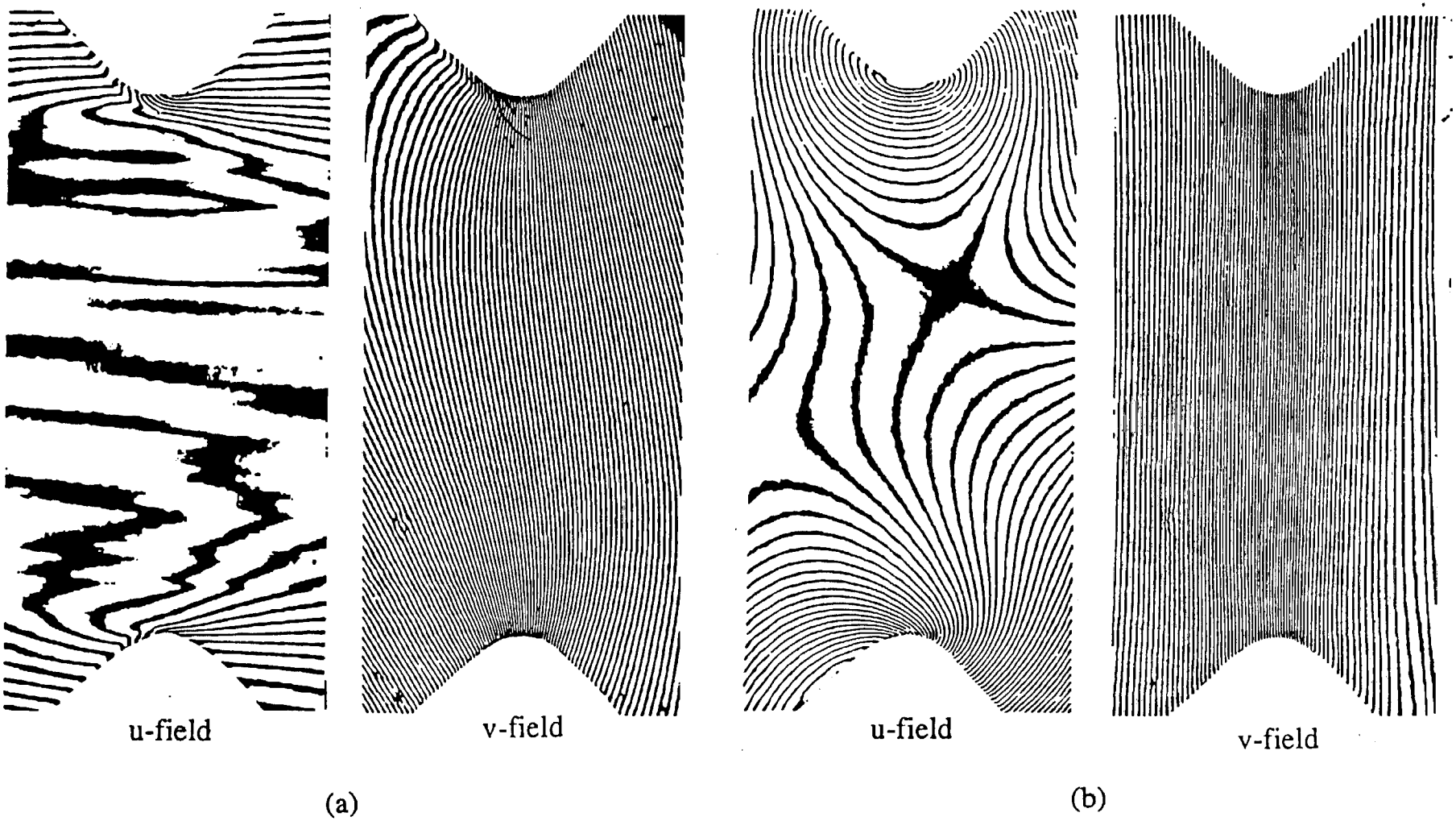

Fig. 4 U- and v-field moire fringe patterns for (a) 0° and (b) 90° graphite-epoxy specimens.

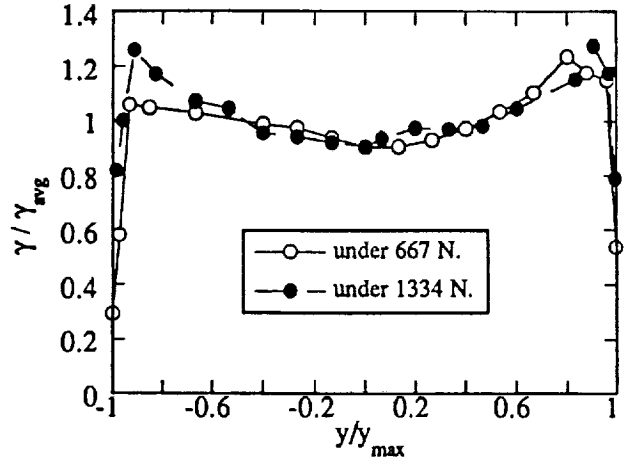

(a)

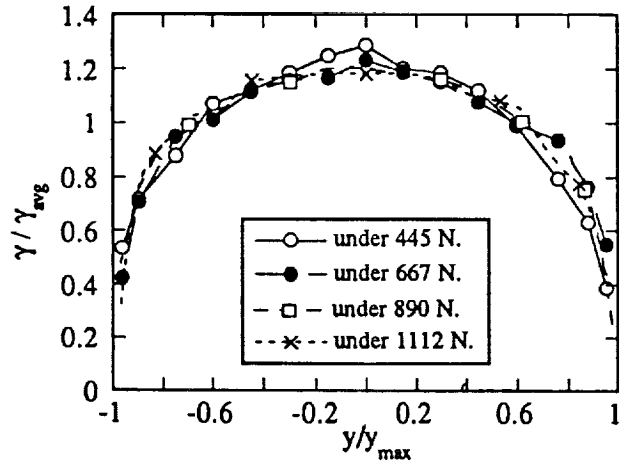

(b)

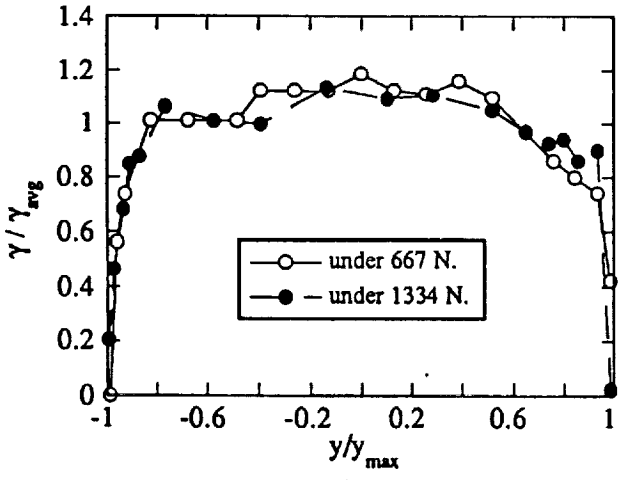

(c)

Fig. 5 Shear strain data across the notches obtained from manual data reduction of moire fringes for (a) 0°, (b) 90° and (c) 0°/90° graphite-epoxy specimens.

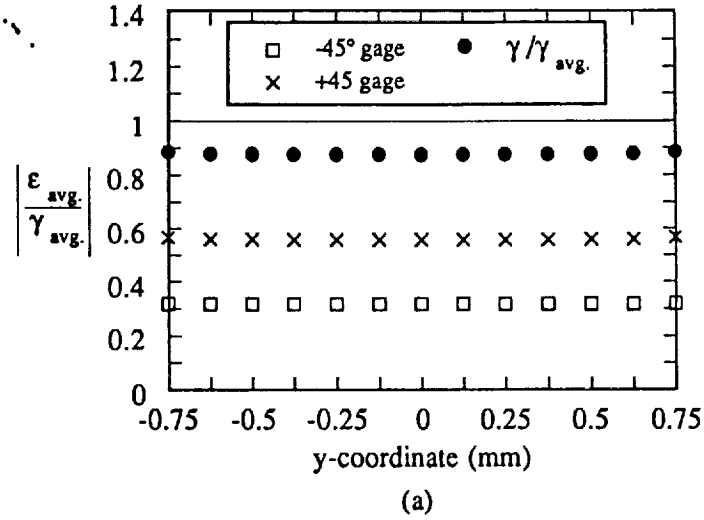

(a)

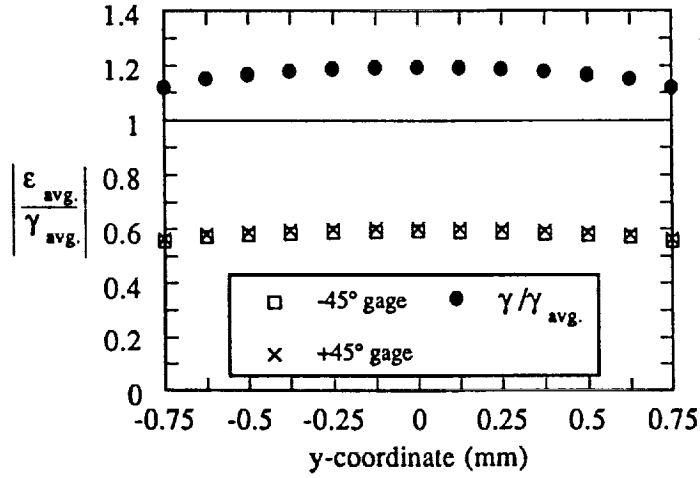

(b)

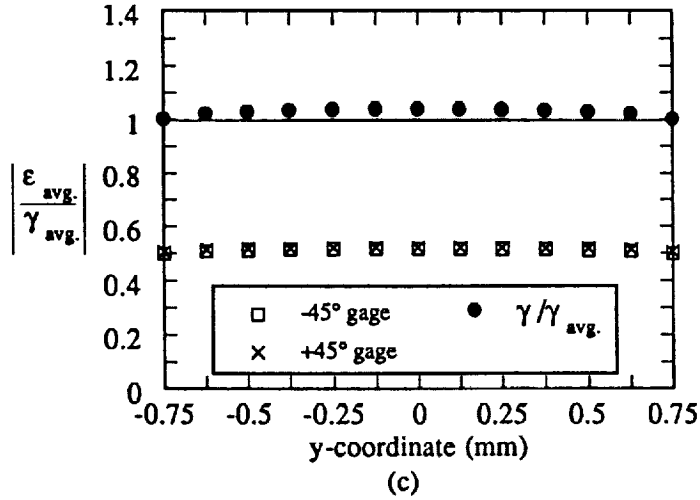

(c)

Fig. 6 Normalized strains of ±45° gages from finite element analysis for (a) 0°, (b) 90° and (c) 0°/90° graphite-epoxy specimens.

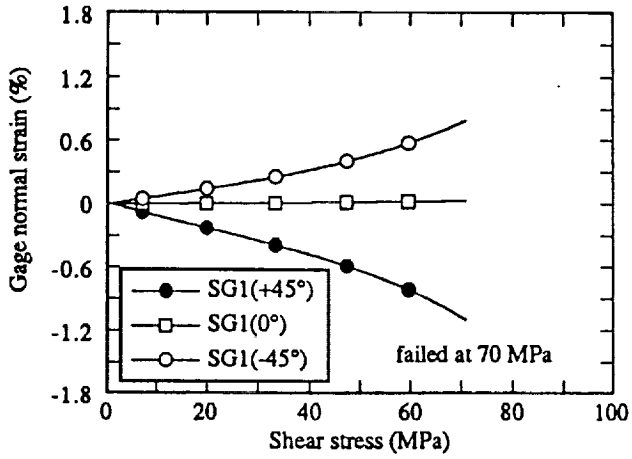

(a)

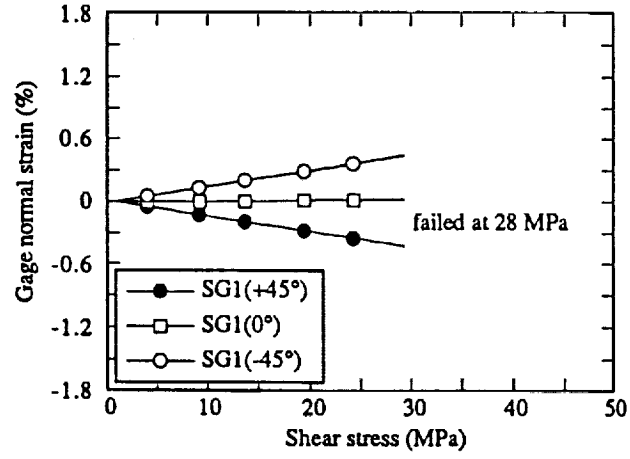

(b)

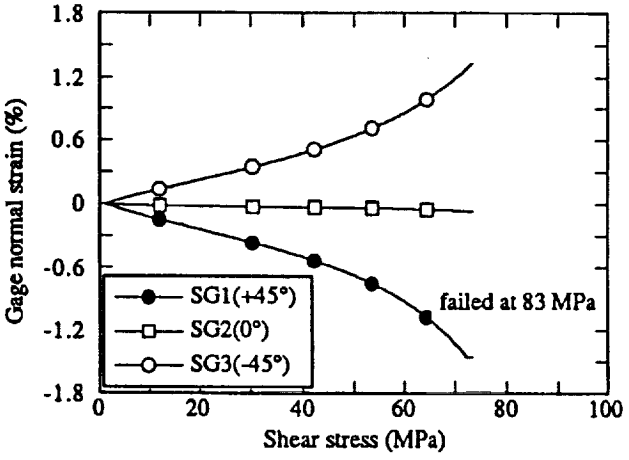

(c)

Fig. 7 Strain vs. stress for typical (a) 0°, (b) 90° and (c) 0°/90° graphite-epoxy specimens. Gages are aligned at ±45° and 0° directions.

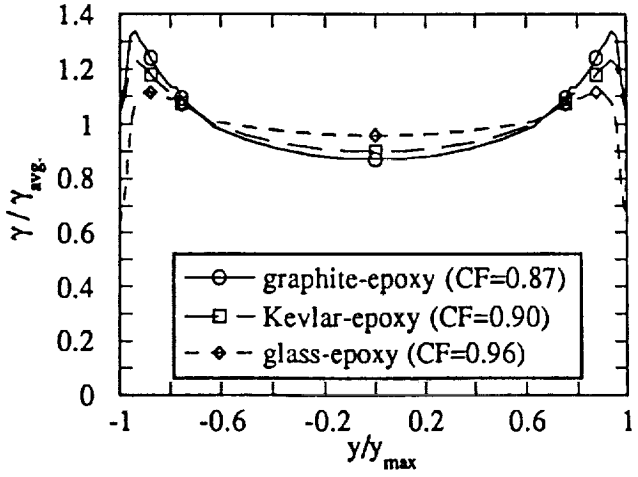

(a)

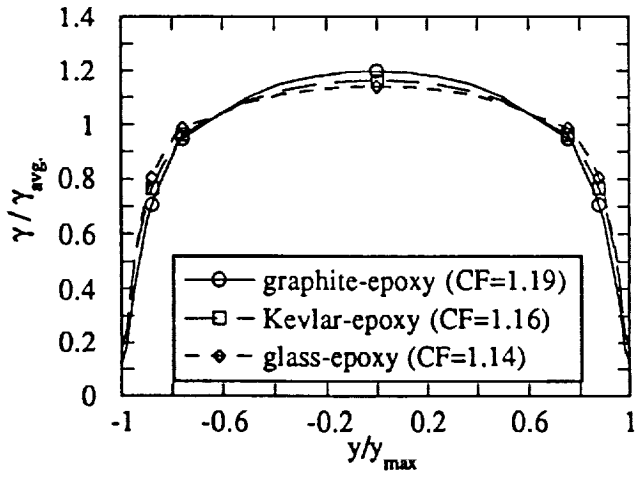

(b)

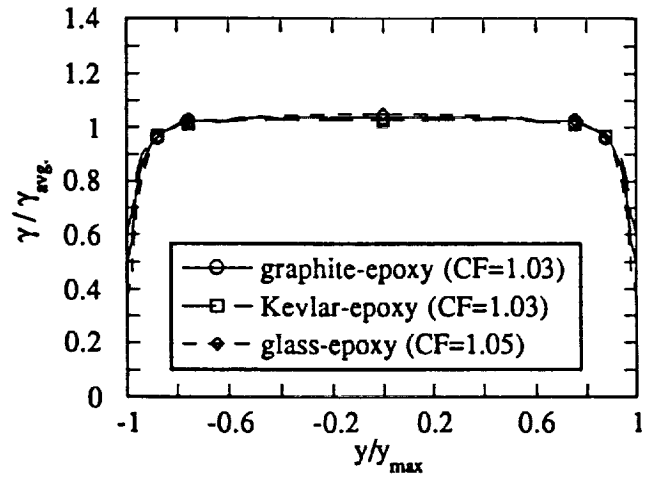

(c)

Fig. 8 Normal and shear strains along the notch axis, normalized with respect to average shear strain, for (a) graphite-epoxy (b) Kevlar-epoxy and (c) glass-epoxy specimens.

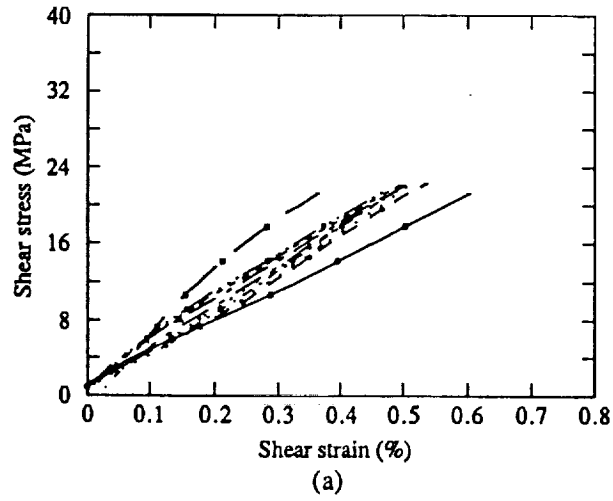

(a)

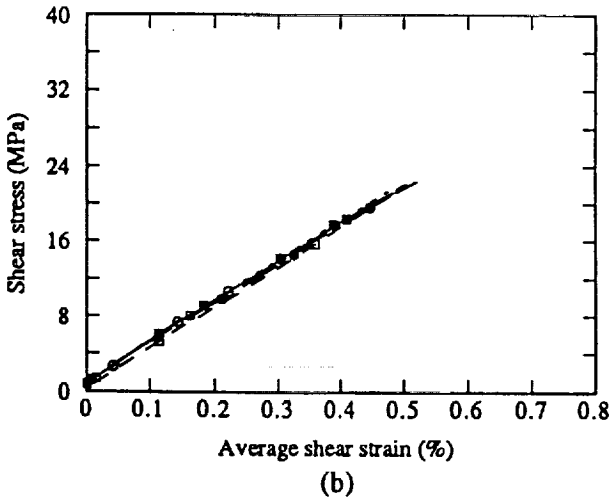

(b)

Fig. 9 (a) Shear stress-strain data for 90° graphite-epoxy loaded in different orientations which were obtained by rotating the specimen about the x,y and z axis. (b) Average of front and back surface shear strains as a function of shear stress.

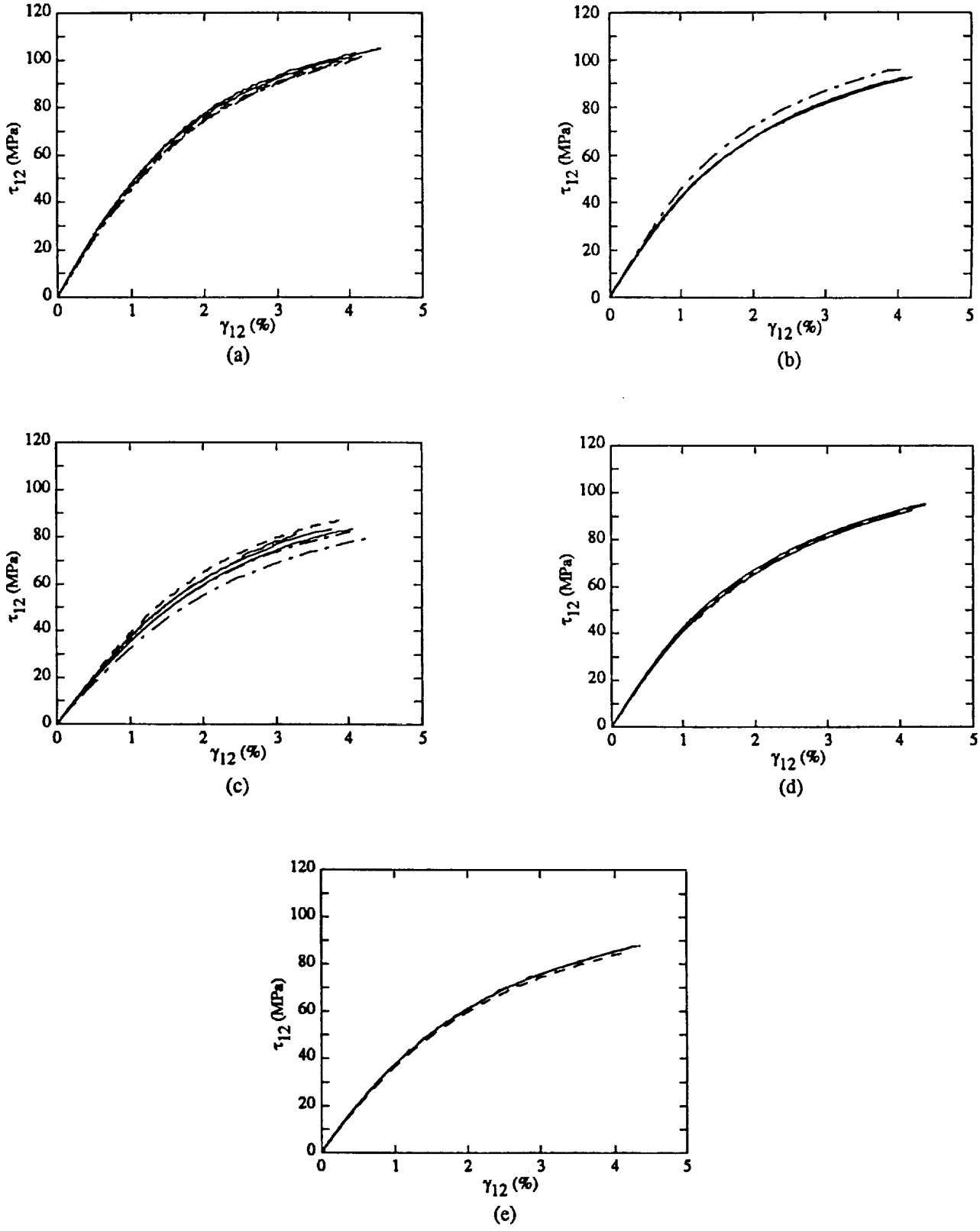

Fig. 10 Average of front and back shear stress-strain data of (a) uniweave $[0/90]_{7s}$, (b) plain weave $[0/90]_{6s}$, (c) plain weave $[0/90]_{2s}$, (d) 5HS $[0/90]_{4s}$ and (e) 8HS $[0/90]_{3s}$ specimens.

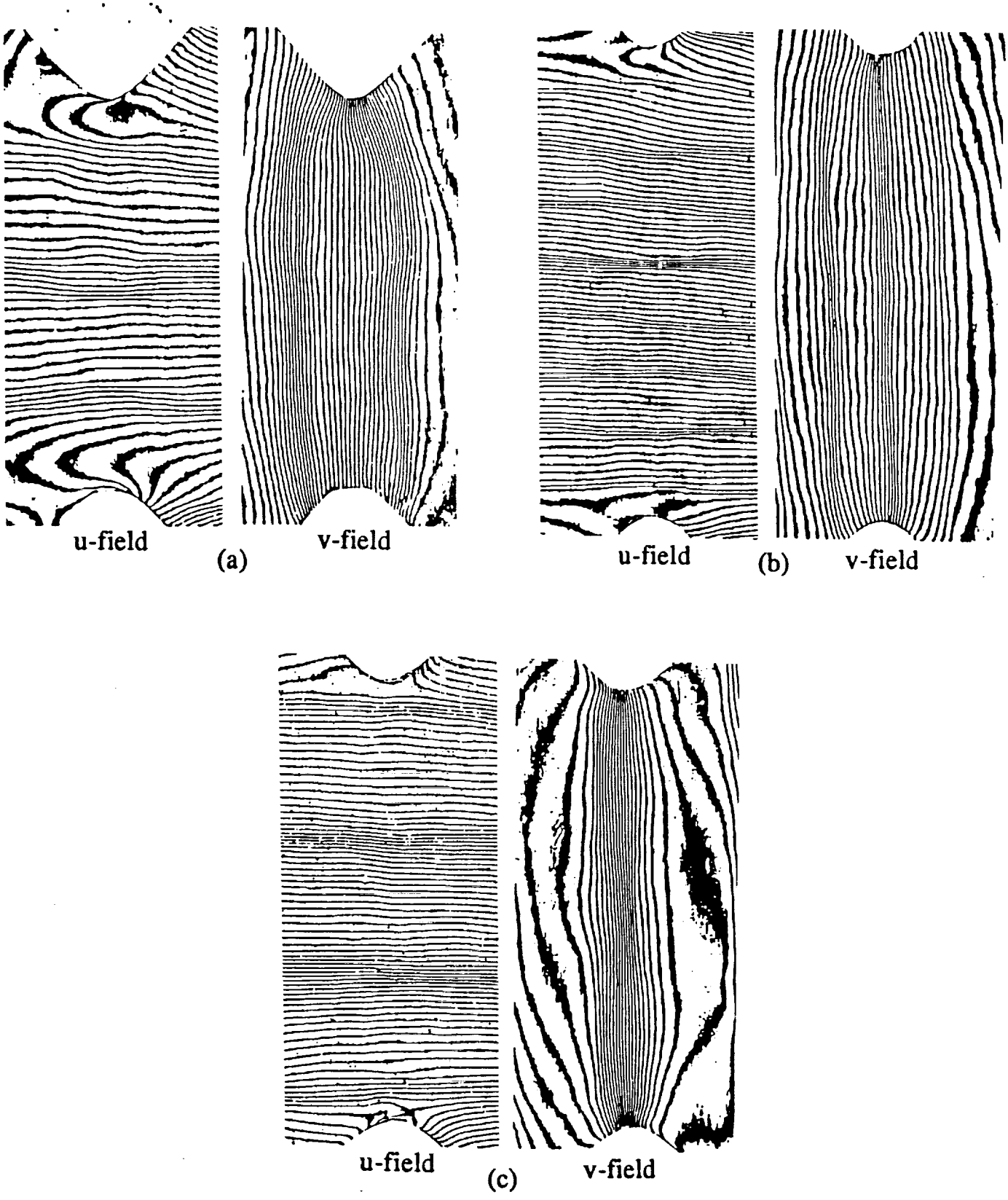

Fig. 11 Typical moire fringe patterns for (a) plain weave $[0/90]_{2s}$, specimen A, (b) 5HS $[0/90]_{4s}$ and (c) plain weave $[0/90]_{2s}$, specimen B.

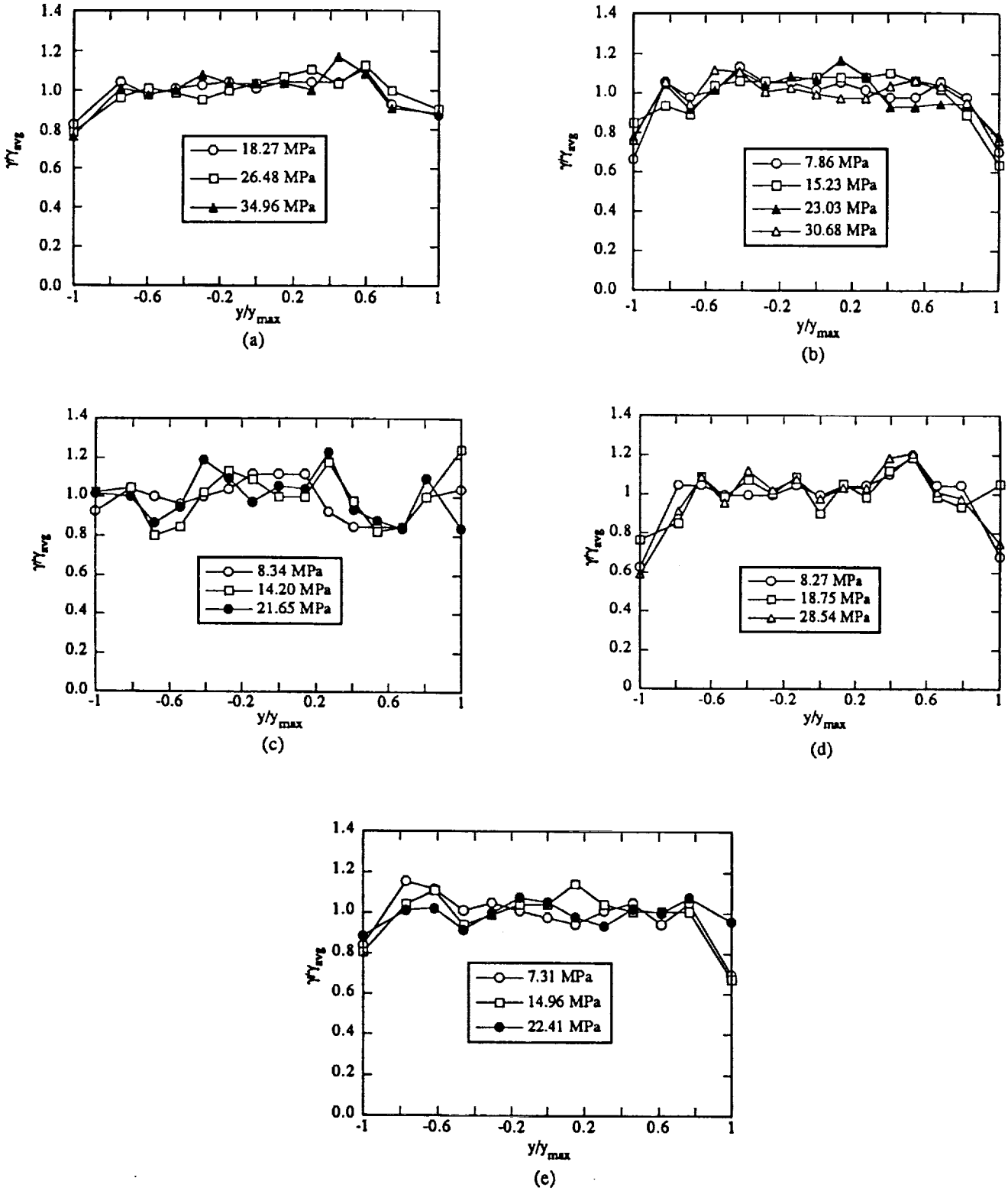

Fig. 12 Shear strains across the notches, normalized with respect to the average shear strain, for (a) uniweave $[0/90]_{7s}$, (b) plain weave $[0/90]_{6s}$, (c) plain weave $[0/90]_{2s}$, (d) 5HS $[0/90]_{4s}$ and (e) 8HS $[0/90]_{3s}$ specimens.

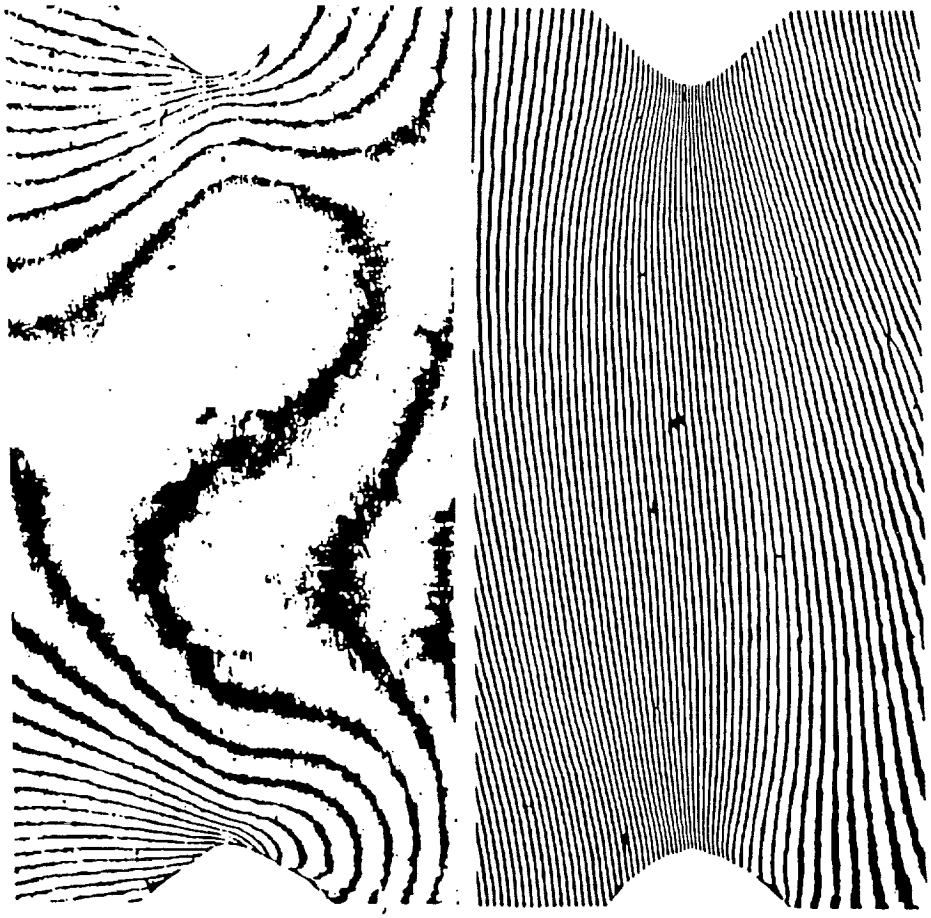

(a)

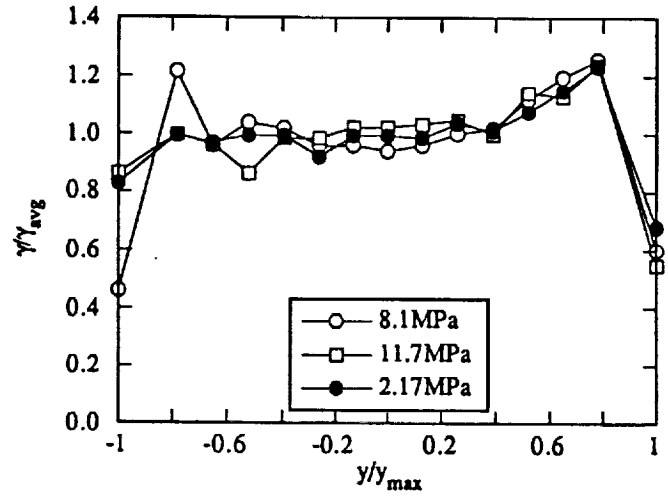

(b)

Fig. 13 (a) Moire fringe patterns of the epoxy based aluminum particulate composite specimens at an applied load of 476N. (b) Shear strains across the notches, normalized with respect to the average shear strain, for epoxy based aluminum particulate composite specimens.

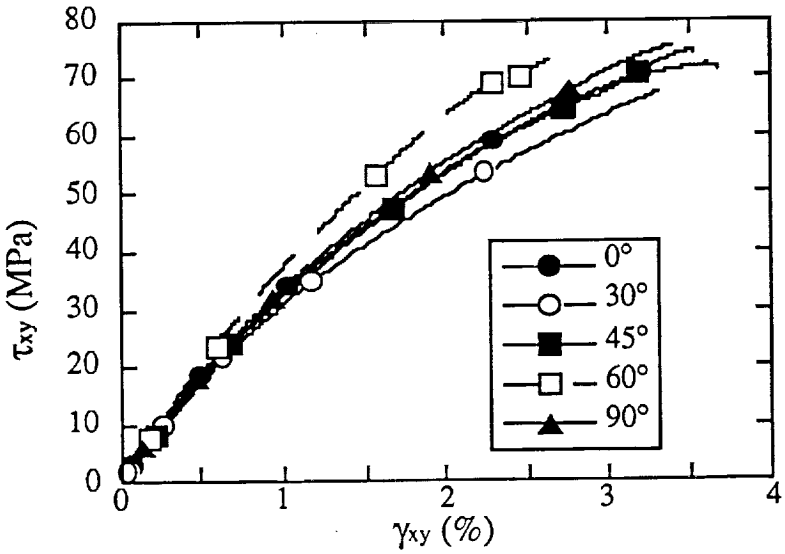

(a)

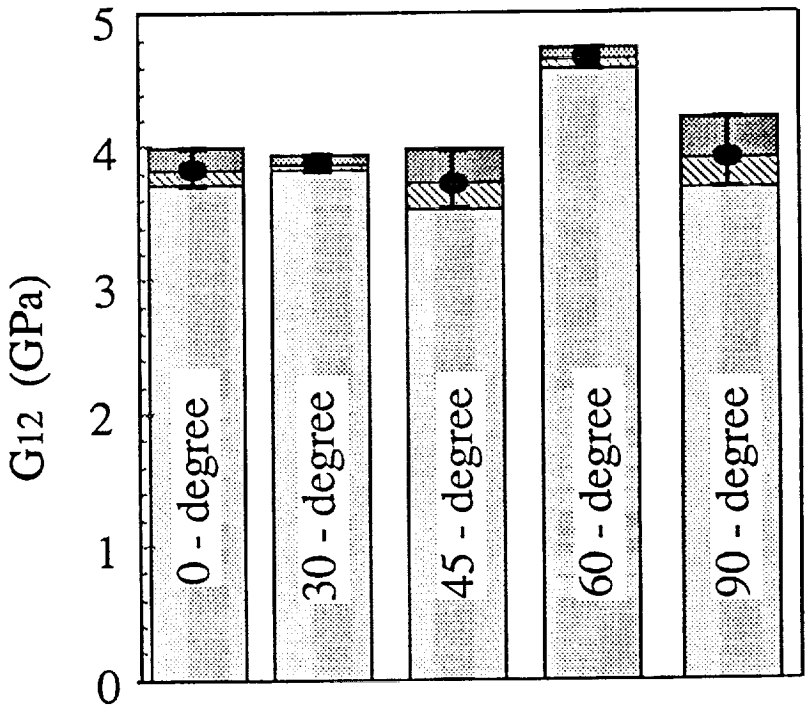

(b)

Fig. 14--(a) Typical shear stress-strain responses, (b) measured shear moduli for different relative orientations of the SMC-28 specimens.

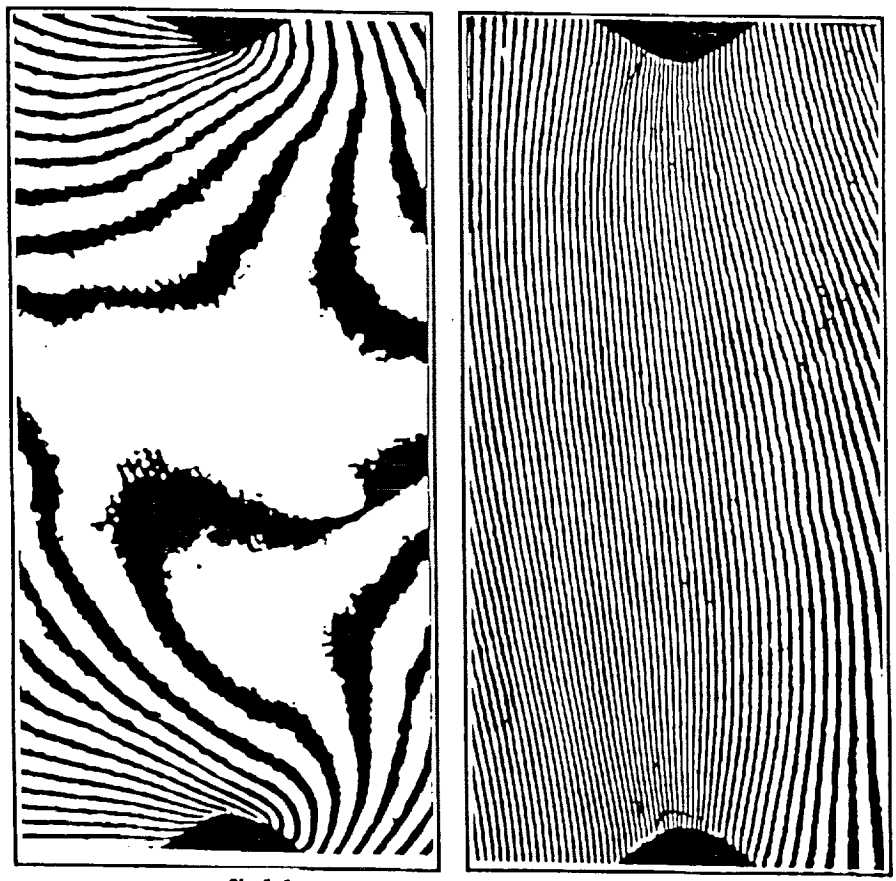

(a)

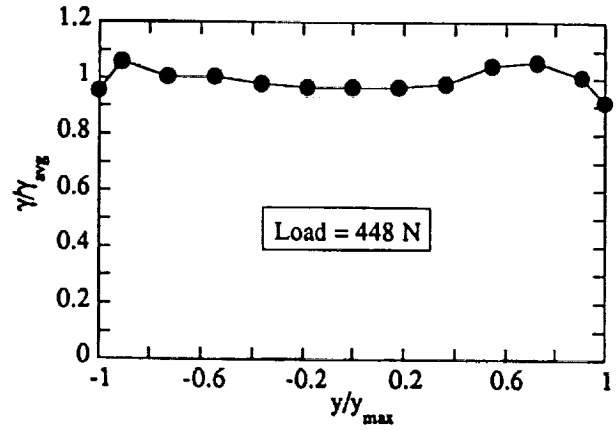

(b)

Fig. 15 (a) Moire fringe patterns, (b) shear strains across the notches, normalized with respect to the average shear strain, of the 0° relative orientation SMC-28 specimen.

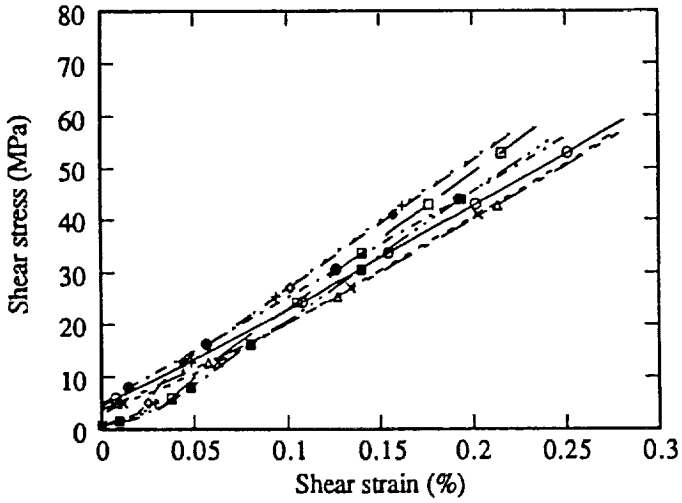

(a)

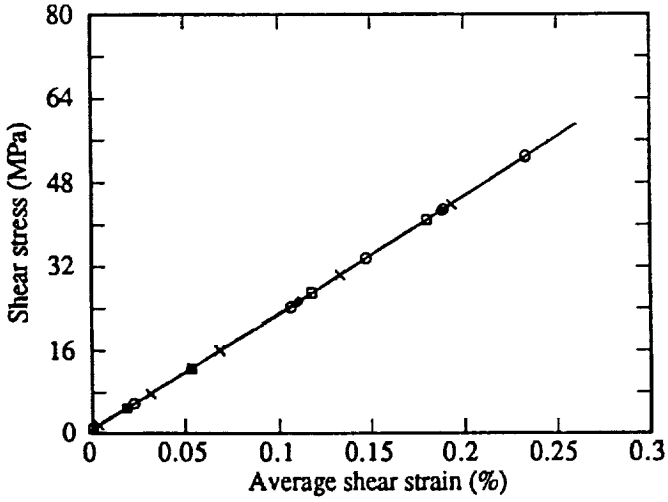

(b)

Fig. 16 (a) Shear stress-strain data for an aluminum alloy specimen loaded in different orientations which were obtained by rotating the specimen about the x,y and z axis. (b) Average of front and back surface shear strains as a function of shear stress.